Design of Anthropomorphic Atherosclerotic Carotid Artery Flow Phantoms for Ultrasound Images

Francesca Galluzzo[1], Filippo Leonardo[1], Alessandro Ceruti[2], Luca De Marchi[1], Cristiana Corsi[1]

[1]DEI-Department of Electrical, Electronic and Information Engineering, "Guglielmo Marconi", University of Bologna, Bologna, Italy

[2]DIN- Department of Industrial Engineering, University of Bologna, Bologna, Italy

Abstract

Carotid artery phantoms (CaPs) can be used as test objects to explore novel ways of enhancing the ultrasound based carotid atherosclerosis diagnosis. To achieve this goal CaPs should be anatomically realistic both in terms of geometry, acoustic and physical properties, and should allow to reproduce different pathological conditions. We propose a framework for designing CaPs of healthy and diseased arteries. To verify the framework effectiveness we constructed three CaPs: healthy, with a hard/soft plaque causing a 30%/65% vessel narrowing. Then we acquired CaPs B-mode images and performed their geometric characterization and echogenicity analysis demonstrating the framework effectiveness at realizing anthropomorphic CaPs at low cost, easily reproducing different atherosclerotic conditions.

1. Introduction

Beside classical applications, carotid artery (CA) flow phantoms can be used as test objects to explore novel ways of enhancing the ultrasound (US) based carotid atherosclerosis diagnosis. To achieve this goal carotid artery phantoms (CaPs) should have anatomically realistic geometry and acoustic, mechanical and physical properties similar to those of real arteries. Moreover, to allow to better understand the onset of vascular diseases with US, they should allow to reproduce different pathological conditions, such as wall hardening, intima-media thickening (IMT), and presence of carotid plaques (CPs) of different morphology and composition. This is particularly important to use the CaP as test object to validate computer aided methods for enhancing carotid atherosclerosis diagnosis, since it is based on the CPs segmentation and composition study [1].

CaPs proposed in literature can be divided in wall-less and walled. In wall-less phantoms the vessel is obtained by realizing an empty channel in a tissue-mimicking material (TMM) block [2, 3] and a blood-mimicking fluid (BMF) is then pumped trough the channel. Although this approach enables the realization of complex geometries, a wall-less phantom is prone to breakage due to BMF infiltrations in the TMM [3] and it makes the production of CPs of different morphology and composition extremely hard. Walled phantoms usually consist in tubular structures made of vessel mimicking material (VMM), embedded in a TMM [4–7] and crossed by a BMF. Due to the difficulties in realizing complex geometries (CA bifurcation and stenosis) on compliant and physically realistic materials, few design methods for anthropomorphic walled phantoms have been proposed that usually exploits lost-materials casting techniques for phantom mold fabrication [8]. To overcome this limitation 3D printing has been exploited to model anthropomorphic geometries on compliant materials [9]. Although several printer technologies exist, a limitation on the printable materials still remains. It means that it is still difficult to exploit 3D printing on versatile VMMs. Furthermore, although these techniques could enable the CPs design they prevent the realization of CPs of different composition.

In this work we propose a framework for easily designing anthropomorphic CaPs overcoming these limitations. It exploits 3D printing to produce an anthropomorphic negative outer vessel mold and several inner cores modeled for reproducing both healthy and diseased arteries. By using this mold a vessel phantom is produced starting from a polyvinyl alcohol (PVA) solution that solidify exposed to several freeze/thaw cycles. The VMM selection is crucial due to the PVA cryogel (PVA-C) characteristics of changing its stiffness based on the freeze/thaw cycles number, duration and temperature, allowing to mimic several atherosclerotic conditions affecting the whole vessel wall or its portions. This design method also allows the accurate design of vessel occlusions eventually embedding additional materials to mimic complex hard and soft CPs. To create a flow CaP the vessel phantom is then embedded in a agar-based TMM and a BMF based on nylon-scatterer solution is pumped through it.

2. Phantom design & realization

The phantom design framework we propose consists in the following steps: (i) the mold design and realization; (ii) the VMM and the vessel phantom realization; (iii) the whole phantom completion, where the TMM and BMF are realized and combined with the vessel phantom.

The first two design chain steps are the design framework core and constitute the main contribute of this work.

Mold design & realization: To realize anthropomorphic phantoms we exploited the 3D printing rapid prototyping technique. By using a computer aided manufacturing (CAM) software we realized a 3D carotid artery model with realistic geometry and then we modeled from it a mold constituted of two parts: a negative outer vessel mold, and an inner core, used to realize the artery lumen (see Figure 1 (a)). As described below, the final vessel phantom is realized by filling the cavity between inner and outer molds with a solution that, once solidified, will take on the artery shape. By using the STL file produced by the CAM software, the 3D printer finally creates the physical mold. The 3D printer used in this work is based on the fused deposition model technique, an additive manufacturing technology that produces a part by laying down plastic (or metallic) fused filaments. Two printing materials have been used: the ABS plastic for the outer mold, and a soluble filament for the inner core. An inner core of soluble material can be easily removed from the final vessel phantom object without damaging it. By using this approach several pathological conditions can be easily reproduced by modifying the inner core model without necessarily change the outer mold. An IMT can be reproduced by changing the ratio between inner and outer mold diameters; the CP of different size and shape presence can be reproduced by accurately modeling the inner core. Figure 1 (b) shows an inner core that we realized to reproduce the CPs presence. A small cavity is created in a carotid bifurcation branch, and then filled with materials suitable to reproduce calcium, fat and the other blood-borne materials responsible of the CPs formation.

VMM realization & and vessel phantom fabrication: Our VMM was realized starting from a PVA solution. This solution is then poured into the mold and undergoes several freeze/thaw cycles to solidify and originate a cryogel. Among the several material proposed to realize VMMs [8], we selected PVA due to its characteristics of changing the PVA-C stiffness by varying the number, temperature and duration of the freeze/thaw cycles. This allows to easily and accurately mimic different vessel phatological conditions without changing the solution and its realization process. Thus we were able to realize phantoms with hard (hyperechoich) and soft (hypoechoic) plaques, by respectively using a PVA-C undergoing more cycles than the rest of the wall, and a mixture of butter and PVA-C un-dergoing less cycles than the wall. PVA molecular weight (mw), hydrolysis degree (hd), polymerization degree (pd) and its percentage in water solution, also influence the final cryogel stiffness, as well as its speed of sound, density, and acoustic attenuation. Based on the results of several studies [4–6, 10] and our experiments, we selected a PVA with pd= $1000 \div 1500$, mw= $85000 \div 124000$ g/mol and hd> 99.3% (Sekisui, Selvol 125) in small concentration. We realized the final VMM solution according to the method proposed in [5]: a mixture in mass percent of 79.5% of deionized water, 10% PVA powder, 10% glycerol for increasing sound speed, 2% Al_2O_3 particles (0.3 μm) acting as scattering particles, and 0.05% benzalkonium chloride (powder > 90%) as an anti-bacterial agent. The solution is realized at 90°C continuosly stirring for 1 hour. Then, after degassing, it is poured in the space between the outer mold and the inner core, and undergoes five freeze/thaw cycles of 12 hour each one at $-20°C/20$ °C. Note that the number of freeze/thaw cycles was tuned according to [10] to obtain a phantom with physical and mechanical properties similar to the ones of real arteries. Thanks to the PVA-C durability a phantom properties time stability of at least one year is ensured.

Similarly, to realize an hard CP phantom, the cavity of the specifically designed inner core (see Figure 1 (b)) was filled with the PVA solution and the mold undergoes two freeze/thaw cycles to let the plaque solidify. Then, all the space between the inner core and the outer mold was filled with the PVA hydrogel and the object undergoes further five freeze/thaw cycles. The resulting object is a phantom with an inclusion harder and more echoic than the rest of the wall. On the other hand, to realize a soft CP phantom we first realize the phantom wall (five freeze/thaw cycles), then liquid butter was injected in the wall (in correspondence of the inner core cavity). After butter solidified in fridge a thin hydrogel layer was injected in the cavity covering the butter and the complete phantom undergoes a further freeze/thaw cycle. The resulting object is a CaP with a soft inclusion that can be assimilated to a lipid core CP.

At the end of these steps robust, compliant, and durable anthropomorphic walled vessel phantoms are produced. Depending on the studies to be conducted and the used US imaging technique, these phantoms can be already used in water bath or simple glycerol solutions [4].

The whole flow phantom completion: To better understand blood flow dynamics, as well as to take into account the effects of the CA surrounding tissues on the US beam propagation a whole CA flow phantom should be realized. To achieve this goal the PVA-C vessel phantom is combined with a TMM and a BMF. The TMM was realized based on the method proposed in [3]. It consists in a solution of 82.97% of deionized water, 11.21% of glycerol (speed of sound tuning), 0.46% of benzalcko-
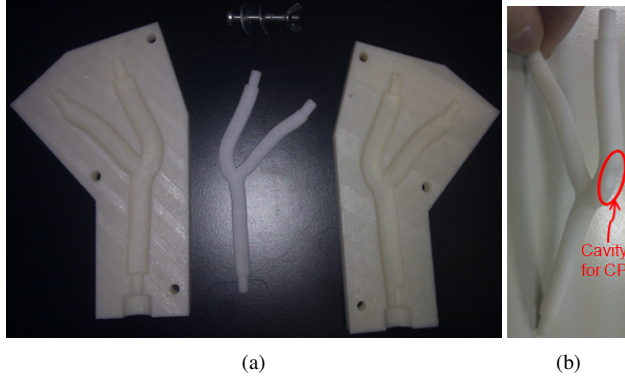
Figure 1: 3D printed phantom mold: (a) negative vessel outer mold and inner core for healthy vessel, (b) inner core with plaque mimicking inclusion cavity

nium cloride (anti-bacterial), 3% of high gel-strenght agar (Sigma-Aldrich, $600 \div 1200$ gm/cm^2), and three types of scatterers mimicking powders: 0.53% of SiC (400 grit), 0.94% of Al$_2$O$_3$ $3\mu m$, 0.88% of Al$_2$O$_3$ $0.3\mu m$. Ingredients are contiously stirred at 96 ± 3°C for 1 hour, then the mixture is let cool and when reaching 42°C it is poured in a box containing the vessel phantom and let solidify at about 20 °C. The BMF was realized according to [3]. It consists in a mixture (percent in mass) of 1.82% of $5\mu m$ Orgasol particles (2001 UDNAT1 Orgasol, ELF Atochem) used as scatterers, 83.86% of distilled water and 10.06% of glycerol to ensure appropriate solution density and speed of sound, 3.36% of Sigma D4786 dextran of average mw 150000D (Sigma Aldrich) to increase solution viscosity, 0.9% of Synperonic A7 surfactant (Croda Health Care).

3. Experimental results

To verify the framework effectiveness we constructed three CaPs: healthy, with hard and soft CPs. Then, by using a ULtrasound Advanced Open Platform for experimental research (ULAOP) [1], we acquired CaPs B-mode images and performed their geometric characterization. Figure 2 shows the realized healthy CaP (a), the acquired B-mode longitudinal images of respectively the healthy (b), hard (c) and soft (d) CP phantoms, and the acquired B-mode images of the radial section of the ICA branches containing the CP for both the hard (e) and soft (f) CPs. From their echogenicity the CPs can be assimilated to a calcific ipo-echoic and a fibro/lipidic CPs. The soft CP phantom also reproduces an IMT in the ICA branch (Figure 2 (d)).

To perform the CaPs geometric characterization we measured both the vessel branches diameters and the wall thickness from B-mode images by using a software measurement tool. To accurately perform these measurements phantom B-mode images were acquired in a water bath,

(a)helthy CaP   (b)healthy CaP longitudinal B-mode

(c)hard CP CaP longitudinal B-mode   (d)soft CP CaP longitudinal B-mode

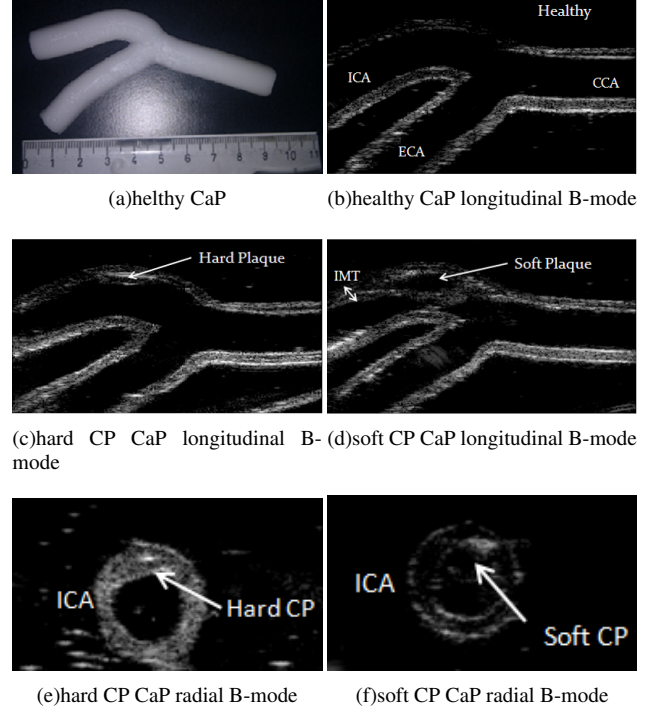(e)hard CP CaP radial B-mode   (f)soft CP CaP radial B-mode

Figure 2: The realized healthy phantom and the acquired B-mode images on the healthy and hard/soft CP phantoms.

Table 1: Phantom and real CA lumen diameters. CCA, ICA and ECA stand for common, internal and external CA.

Internal Diamter	Real Carotid Artery dx/sx (mm)	Phantom Caliper Measurements (mm)	Phantom B-mode image measurements
CCA	$7.56 \pm 1.46/7.71 \pm 1.13$	7.8 ± 0.025	$7.21 \div 7.63$
ICA	$6.38 \pm 1.22/6.85 \pm 1.72$	7.7 ± 0.025	$6.88 \div 7.57$
ECA	$5.92 \pm 1.35/5.72 \pm 1.23$	6.8 ± 0.025	$6.38 \div 6.75$

while the TMM echogenicity was examined separately. Phantom dimensions, where then verified by means of a caliper and compared with values of in-vivo measurements. Table 1 shows the CaP lumen diameters along with the corresponding human CA typical values. Ranges refers to the measurements on the three CaPs.

The realized phantoms accurately mimic the real CA with lumen diameters comparable to the ones of real arteries. The similarity between the common CA (CCA) and internal CA (ICA) diameters, higher than the one existing in human arteries, is due to the necessity of simplify the mold design starting from a geometrical CAM model. To overcome this limitation we are designing the realization of a 3D mold model from the CA segmentation of real MRI images. The phantoms wall thickness, measured from B-mode images, ranged between $1.2 \div 2.12$ mm for the normal wall and between $2 \div 4.63$ mm in presence of stenosis, which are in good agreement with real wall thickness values ($\approx$ 1mm, $> 1 \div 4$mm). The hard CP ($\approx$ 2mm
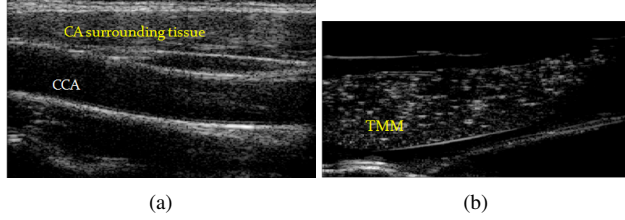
(a)   (b)

Figure 3: Real CA (a) and realized TMM (b) US images.

Table 2: State of art CaP realization methods comparison

Method	Walled	anthropomorphic	Variable Stiffness	Hard/Soft	Mixed	TMM	BMF	RP
Present	√	√	√	√	√	√	√	√
Widman'13 [4]	√	−	√	√	−	√	√	−
Lai'13 [9]	√	√	−	−	−	√	√	√
Ramnarine'14 [5]	√	−	√	√	−	−	√	−
Boekhhoven'14 [6]	√	−	√	−	−	−	−	−
Poepping'04 [8]	√	√	−	√	−	√	√	−
Majdouline14 [7]	√	−	√	√	−	−	−	−
Ramnarine'01 [3]	−	−	−	−	−	√	√	−
Dineley'06 [11]	√	−	√	−	−	√	−	−
Rickey'95 [8]	−	−	−	−	−	√	−	−
Potter'08 [12]	√	−	−	−	−	−	√	−
Fenster'06 [2]	−	−	−	√	−	−	√	−

thick) causes of a 27% vessel narrowing corresponding to a medium import pathological condition, while the soft CP (4.6 mm thick) is responsible of 65% stenosis corresponding to a serious pathological condition. Finally, figure 3 shows a detail of the realized embedding TMM (a) and a B-mode image of a real CA (b) for comparison: a good echogenicity agreement between our TMM and the in-vivo tissues can be observed.

To evaluate our approach *w.r.t.* the state of the art we compared it with several US-aimed CaPs realization methods proposed in the last twenty years. Our comparison, based on the main characteristics that a flow phantom should have is shown in Table 2. It can be observed that our method is the most complete since it allows to obtain an anthropomorphic walled phantoms: (i) extremely flexible in terms of applicability, since its acoustic and mechanical properties can be easily tuned without changing the phantom material; (ii) it enables the study of the onset of cardiovascular disease, since it allows to easily reproduce CPs of different size, geometry and composition, as well as IMT; (iii) combined with the realized TMM and BMF provides an extremely realistic US acquisition setup and enables different US-based investigations.

4. Conclusions

In this work a framework for realizing anthropomorphic CaPs for US imaging was proposed. By exploting 3D printing for mold realization and an extremely versatile VMM it allows to easily fabricate anthropomorphic CaPs at low cost, reproducing different atherosclerotic conditions. The framework can be further developed to support patient specific modeling.

Acknowledgements

References

[1] Galluzzo F, Corsi C, Morizzo C, De Marchi L, Testoni N, Speciale N, Masetti G. Capsu: A completely automated method for carotid plaques segmentation in ultrasound images. In CinC, 2014. IEEE, 2014; 309–312.

[2] Fenster A, Blake C, Gyacskov I, Landry A, Spence J. 3d ultrasound analysis of carotid plaque volume and surface morphology. Ultrasonics 2006;44:e153–e157.

[3] Ramnarine KV, Anderson T, Hoskins PR. Construction and geometric stability of physiological flow rate wall-less stenosis phantoms. UMB 2001;27(2):245–250.

[4] Widman E, Caidahl K, Heyde B, D'hooge J, Larsson M. Speckle tracking strain estimation of a carotid artery plaque phantom-validation via sonomicrometry. In IUS, 2013 IEEE. IEEE, 2013; 1757–1760.

[5] Ramnarine KV, Garrard JW, Dexter K, Nduwayo S, Panerai RB, Robinson TG. Shear wave elastography assessment of carotid plaque stiffness: in vitro reproducibility study. UMB 2014;40(1):200–209.

[6] Boekhoven RW, Rutten MC, van Sambeek MR, van de Vosse FN, Lopata RG. Echo-computed tomography strain imaging of healthy and diseased carotid specimens. UMB 2014;40(6):1329–1342.

[7] Majdouline Y, Ohayon J, Keshavarz-Motamed Z, Cardinal MHR, Garcia D, Allard L, Lerouge S, Arsenault F, Soulez G, Cloutier G. Endovascular shear strain elastography for the detection and characterization of the severity of atherosclerotic plaques: In vitro validation and in vivo evaluation. UMB 2014;40(5):890–903.

[8] Poepping TL, Nikolov HN, Thorne ML, Holdsworth DW. A thin-walled carotid vessel phantom for doppler ultrasound flow studies. UMB 2004;30(8):1067–1078.

[9] Lai SS, Yiu BY, Poon AK, Alfred C. Design of anthropomorphic flow phantoms based on rapid prototyping of compliant vessel geometries. UMB 2013;39(9):1654–1664.

[10] Fromageau J, Gennisson JL, Schmitt C, Maurice RL, Mongrain R, Cloutier G, et al. Estimation of polyvinyl alcohol cryogel mechanical properties with four ultrasound elastography methods and comparison with gold standard testings. IEEE TUFFC 2007;54(3):498–509.

[11] Dineley J, Meagher S, Poepping T, McDicken W, Hoskins P. Design and characterisation of a wall motion phantom. UMB 2006;32(9):1349–1357.

[12] Potter K, Reed CJ, Green DJ, Hankey GJ, Arnolda LF. Ultrasound settings significantly alter arterial lumen and wall thickness measurements. Cardiovasc Ultras 2008;6(1):6.

Address for correspondence:

Francesca Galluzzo

University of Bologna-DEI, V.le Risorgimento, 2, 40136, Bologna, Italy. francesca.galluzzo@unibo.it